Lejarazu-Larrañaga *et al. Energy Mater.* **2025**, *5*, 500044
DOI: 10.20517/energymater.2024.122

Energy Materials

Article

Open Access

Check for updates

Tuning the ion-transport nanochannels of sulfonated poly(ether ether ketone) membranes for efficient aqueous organic redox flow battery

Amaia Lejarazu-Larrañaga[1], Eduardo Sánchez-Díez[1], Yan Zhang[1], Ivan Bobrikov[1], Nagore Ortiz-Vitoriano[1,2], Nerea Marquinez[1], Fengjing Jiang[1,*]

[1]Centre for Cooperative Research on Alternative Energies (CIC energiGUNE), Basque Research and Technology Alliance (BRTA), Alava Technology Park, Vitoria-Gasteiz 01510, Spain.
[2]Ikerbasque, Basque Foundation for Science, Bilbao 48013, Spain.

***Correspondence to:** Prof./Dr. Fengjing Jiang, Centre for Cooperative Research on Alternative Energies (CIC energiGUNE), Basque Research and Technology Alliance (BRTA), Alava Technology Park, Albert Einstein 48, Vitoria-Gasteiz 01510, Spain. E-mail: fjiang@cicenergigune.com

How to cite this article: Lejarazu-Larrañaga, A.; Sánchez-Díez, E.; Zhang, Y.; Bobrikov, I.; Ortiz-Vitoriano, N.; Marquinez, N.; Jiang, F. Tuning the ion-transport nanochannels of sulfonated poly(ether ether ketone) membranes for efficient aqueous organic redox flow battery. *Energy Mater.* **2025**, *5*, 500044. https://dx.doi.org/10.20517/energymater.2024.122

Received: 14 Aug 2024 **First Decision:** 9 Sep 2024 **Revised:** 30 Sep 2024 **Accepted:** 24 Oct 2024 **Published:** 19 Feb 2025

Academic Editor: Meicheng Li **Copy Editor:** Fangling Lan **Production Editor:** Fangling Lan

Abstract

Sulfonated poly(ether ether ketone) (SPEEK) is a potential low-cost candidate to replace fluorine-based Nafion membranes in some redox flow batteries (RFBs). In this work, the ionic conductivity of SPEEK membranes is increased almost fourfold by conducting a well-controlled irreversible swelling of the membrane. Atomic Force Microscopy images and small-angle X-ray Scattering curves effectively demonstrate that the size of the hydrophilic nanochannels in the swollen membranes can be precisely tuned by simply varying the solvent concentration. The modified SPEEK membrane (SPEEK45) is applied in an aqueous organic/organometallic RFB, using 1,1′-bis(3-sulfonatopropyl)-4,4′-bipyridinium (SPr_2V) and ferrocyanide salts as anodic and cathodic materials, respectively. The boosted conductivity of the modified SPEEK membrane enables higher energy efficiencies than in the case of the Nafion membrane (N212) at various current densities. In addition, a 200-cycle charging-discharging test is carried out to evaluate the long-term stability of the modified SPEEK membrane. The results show that SPEEK45 exhibits higher energy efficiency than N212 (70.8% and 65.4% at 60 mA cm^{-2}, respectively), with comparable capacity retention. The well-controlled swelling method proves to be a promising and innovative membrane technology for promoting ion conductivities of membranes used for various RFBs.

Keywords: Flow battery, non-fluorinated, membrane, ion-transport channels, aqueous organic redox flow battery

INTRODUCTION

Batteries are crucial elements to mitigate the intermittent nature of renewable energy sources, and thus, they play a pivotal role in energy transition. Redox flow batteries (RFBs) stand as prime candidates for future large-scale stationary electrochemical energy storage. This is primarily due to their ability to store energy over extended periods, and their notably flexible design, which results from their unique capacity to decouple energy and power[1].

In the cell stack, a membrane is used to prevent the mixing of the negative and positive electrolytes and to close the electrical circuit through the transport of charge-balancing ions. Perfluorinated membranes such as Nafion represent the state-of-the-art (SoA) separators for RFBs. However, the European Chemicals Agency (ECHA) has recently released a restriction proposal that could prospectively ban the manufacture and use of perfluorinated materials[2]. In addition, the high cost of Nafion membranes (500-700 \$ m^{-2}), which represents almost 40% of the total cost of the cell stack, is a critical bottleneck for the widespread industrialization of RFBs[3,4]. These conditions determine the future of SoA membranes, prompting researchers to explore alternative polymers.

Sulfonated polyether ether ketone (SPEEK) is a promising material to replace perfluorinated membranes, considering its low cost, chemical and mechanical stability and ease of processing[5,6]. Indeed, the cost of SPEEK membranes could approach 40 \$ m^{-2}, which represents just 8% of the price of Nafion counterparts, making them remarkably attractive from the economic point of view[7,8].

Differences in the microstructure between SPEEK and perfluorinated membrane led to distinct transport properties[9]. For dense SPEEK membranes with a moderate sulfonation degree, the lack of a clear separation between hydrophilic and hydrophobic phases leads to the formation of narrow ion transport channels with multiple ends. This structural complexity restricts ion transport efficiency[10-12]. Introducing a larger number of fixed charges is a well-known strategy to enlarge the hydrophilic domains of the membranes. However, a high concentration of fixed charges would lead to an excessive swelling of the membrane, compromising its mechanical stability in the electrolyte. Besides, it has been demonstrated that in highly oxidative environments, the electron-withdrawing effect of SO_3^- groups reduces the chemical stability of the polymer backbone[13,14].

In contrast, microporous structures can serve to create wide and well-connected ion transport nanochannels, without compromising the chemical stability of the membrane[15]. Microporous membranes can be relatively easily prepared by several methods, such as via non-solvent induced phase separation (NIPS), using hydrophilic polymers of intrinsic microporosity (PIMs)[16,17], or adding washable pore-forming templates [phenolphthalein[18], SiO_2 solid spheres[19], polyethylene glycol (PEG)[20], or mixed templates, such as a combination of PEG and dibutyl phthalate[21]]. In previous works, the ion transport efficiency of SPEEK membranes was successfully improved by blending with metal-organic frameworks[22] and PIMs[23]. In addition, strengthening the phase separation by promoting the rearrangement of polymer chains has been demonstrated to enhance the ionic conductivity in SPEEK membranes. Such effect was achieved by a hydrothermal treatment in[11], which, in turn, led to the degradation of the mechanical stability. The controlled swelling method is a different avenue to construct well-connected ion transport nanochannels in polymer membranes including both ionic and non-ionic types. In this method, the dense membrane is initially swollen in a solvent/non-solvent bath and then rapidly immobilized in a non-solvent bath. This process induces irreversible swelling of the polymer chains, enlarging and enhancing the connectivity of the hydrophilic domains, thereby promoting faster ion transport[24,25]. Since water typically acts as the non-solvent in this method, it is quite cost-effective. Thus, this approach allows us to produce

membranes that offer a well-balanced performance at a lower cost.

In this work, dense SPEEK membranes were prepared and immersed in a solvent/non-solvent bath to promote their controllable irreversible swelling, aiming to enhance the ionic conductivity. The size of the ion transport nanochannels in wet conditions was investigated by atomic force microscopy (AFM) and small-angle X-ray scattering (SAXS). The effect of the treatment on the membrane microstructure was analyzed and correlated with its transport properties. Membranes were tested in a symmetric aqueous organic/organometallic RFB, using 1,1′-bis(3-sulfonatopropyl)-4,4′-bipyridinium (SPr_2V) as anodic active material, and sodium and potassium ferrocyanide as cathodic active materials. Such redox-active molecules are based on abundant elements and can be obtained at a considerably low cost, making it worth having "sleeping" materials in the symmetric configuration[26]. Overall, solvent controlled swelling method is presented as an attractive strategy to tune the ion transport nanochannels of SPEEK membranes, enabling higher energy efficiencies (EEs).

EXPERIMENTAL

Chemical reagents and membranes

SPEEK polymer in K^+ form (1.65 meq g^{-1} exchange capacity, 57% sulfonation degree) from Quintech and dimethyl acetamide 99% (DMAc) from Sigma-Aldrich were used for the preparation of the membranes. Commercial Nafion™ N212 membrane (50.8 μm thick as received, 55 μm in water-swollen state) was purchased from Ion Power, Inc. Sodium ferrocyanide decahydrate ($Na_4[Fe(CN)]_6 \cdot 10H_2O$) from Sigma-Aldrich, potassium ferrocyanide trihydrate ($K_4[Fe(CN)]_6 \cdot 3H_2O$) from Across Organic, and 1,1′-bis(3-sulfonatopropyl)-4,4′-bipyridinium (SPr_2V) were used as redox-active species. The synthesis of SPr_2V and the solubility of the redox-active materials are detailed in Supplementary Material S1. NH_4Cl from Thermo Fisher was used as a supporting electrolyte. Distilled water was used throughout the experiments.

SPEEK membrane preparation

SPEEK was dissolved in DMAc (15% w/v) by heating the mixture at 60 °C and stirring for 3 h. The resulting solution was kept without stirring overnight to release air bubbles. The mixture was then cast on a clean glass plate with a thickness of 0.5 mm using a doctor blade. Afterward, the solvent was completely evaporated in a vacuum oven at 80 °C. The dry SPEEK membranes were peeled off from the plate in a water bath. The average thickness of water-swollen SPEEK membranes was 57 ± 6 μm. The original dense SPEEK membrane was named SPEEK0 hereafter. The solvent-induced swelling method was used to finely modify the ion transport nanochannel structure in SPEEK0 membranes. For that purpose, SPEEK membranes were immersed in a mixture of DMAc and water, containing different DMAc concentrations of 40%, 45%, and 50% (v/v), respectively, for 3 h at 30 °C. Afterward, the membrane was immersed in a water bath to completely remove the solvent, allowing for the solidification of the membrane structure. The solvent-treated membranes were named according to the percentage of DMAc used (% v/v), e.g., SPEEK45 for a 45% v/v DMAc solution. The modified membranes were stored in wet conditions to avoid the shrinkage of the ion-transport channels.

Characterization of ion transport channels

The morphology of the nanophase separation and the distribution of the ionic domains of swollen SPEEK membranes were analyzed by AFM. All the topography images presented in this work were recorded with Agilent 5500 AFM by applying tapping operational mode. Non-coated silicon cantilevers (App Nano) with a nominal spring constant of about 40 N m^{-1} and a resonant frequency of 270 kHz were used. To avoid pore constriction, the membranes were prevented from drying during the analyses. For that purpose, the water-swollen membranes were immersed in glycerol for 24 h before the analysis. The excess glycerol was removed from the membrane surface with a tissue prior to the analysis. The high hydrophilicity and low

vapor pressure of glycerol make this compound very useful for preserving the porous structure of membranes[27].

SAXS was employed as a complementary technique to study the nanophase separation structure of the membranes. A Bruker Nanostar instrument was used, composed of a CuK-α source (λ ≈ 1.542 Å) operating at 40 mA and 35 kV, three pinhole collimators, evacuated beam path and a Vantec 2000 2D detector of active surface area 14 mm × 14 mm and 2,048 × 2,048 pixels. A nickel foil was used to filter out Kβ from the Cu tube source. The sample-to-detector distance of 108 cm has been used, enabling the determination of the X-ray scattering intensity $I(q)$ in the range of momentum transfer $0.01 < q < 0.3$ Å^{-1} ($0.1 < q < 3$ nm^{-1}). Water-swollen membrane samples (4 mm diameter) were loaded to the sample holder and a small amount of distilled water (5 μL) was added to keep the membrane in wet conditions. The sample holder was properly sealed using Kapton tape to avoid water evaporation during the measurements. The exposure time for each sample was 1 h. The measured intensity has then been corrected for all the relevant factors including sample transmission. The scattering from the sample holder has been subtracted. Then, the q values corresponding to the ionomer scattering peaks were graphically determined by linear extrapolation, and the lattice plane spacing (d distance) was calculated from Bragg´s law:

$$d = \frac{2\pi}{q} \tag{1}$$

The size of the ionomer clusters was estimated based on approximations described before in[28] (see Supplementary Equations 1-4).

Membrane density, water absorption and apparent porosity

Dry membrane density was calculated from the dry mass and volume (i.e., the product of the membrane area and the membrane thickness) of the membrane. For water absorption studies, the membranes were swollen in water for at least 24 h, and afterward, the membrane weight, size and thickness were recorded. Subsequently, the membranes were dried in a vacuum oven at 80 °C for at least 48 h, and the weight, size and thickness of dry membranes were measured. Water absorption (mass) (Δm) was calculated from the weight difference between the swollen and the dry membrane (Equation 2) and apparent porosity was calculated considering the volume change of swollen and dry states of the membranes (Equation 3)[29],

$$\Delta m = \frac{W_w - W_d}{W_d} \tag{2}$$

$$App.porosity = \frac{W_w - W_d}{\rho_w V_w} \times 100\% \tag{3}$$

where W_w and W_d (g) are the mass of the wet and dry membranes, respectively, ρ_w (g cm^3) is the density of water, and V_w (cm^3) is the volume of the wet membrane.

Permeability and selectivity of the membranes to the redox-active species

The permeability of a membrane towards a specific molecule is usually studied by measuring the diffusion constant in an H-shaped cell [Supplementary Figure 1]. The membrane under study (A = 5.31 cm^2) was placed between the two compartments. One of the half cells (i.e., the feed side) was filled with a 0.1 M aqueous solution of the redox-active material in an uncharged state, dissolved in NaCl, while the other compartment (i.e., the diluted side) was filled with an aqueous solution of NaCl. The concentration of NaCl in the feed side was varied to maintain the same ionic strength in both compartments (1 M in the case of SPr_2V and 0.75 M in the case of ferrocyanide salts). In the case of the diluted compartment, the

concentration of NaCl was kept as 1 M in all the experiments. The solutions were stirred during the experiments to avoid concentration polarization effects. The concentration evolution of the active materials in the diluted compartment was monitored by using an ultraviolet-visible (UV-Vis) spectrophotometer (Varian Cary 5000). At the pseudo-steady state, the permeability of redox-active molecules through the membrane was calculated from their mass balances and Fick´s first law. Using Supplementary Equations 1-7 in Supplementary Material, the permeability or the diffusion coefficient of the redox molecules through the membrane, P (cm^2 s^{-1}), can be calculated as follows[30-32],

$$P = \frac{\Delta \ln\left(1 - \frac{2C_D}{C_0}\right)\left(-\frac{V_0 L}{2A}\right)}{\Delta t} \quad (4)$$

where C_D (mol cm^{-3}) is the active material concentration measured at the diluted side at time t; C_0 (mol cm^{-3}) is the initial active material concentration on the feed side (1 × 10^4 mol cm^{-3}, in this case); V_0 (cm^3) is the initial volume of either the diluted or feed sides (18 cm^3). A (cm^2) is the effective area of the membrane (5.31 cm^2); L (cm) is the thickness of the membrane, and t (s) is the experimental time.

The selectivity to redox-active materials (S, mS s cm^{-3}) was then calculated as the ratio between ionic conductivity and permeability of the redox-active molecules.

$$S = \frac{\sigma}{P} \quad (5)$$

Tensile strength tests

Mechanical properties were tested using a 34SC-5 Single Column dynamometer from Instron equipped with a 100 N load cell. All samples were kept in water and then cut into 4 × 1 cm^2 pieces, following an internal standard procedure. Strain was determined from the crosshead separation in reference to a 10 mm initial length, and stress was defined as the ratio between the force (load) and the cross-sectional area tested. The tensile strength was determined from the stress value at the maximum load before fracture. At least five samples from each membrane were tested and the average values were obtained.

Ionic conductivity and single cell tests

Figure 1 shows a schematic illustration of the symmetric aqueous organic/organometallic RFB. SPr_2V served as the active material in the anode half-cell, and $[Fe(CN)_6]^{4-}$ provided the active material in the cathode half-cell (Na^+ or K^+ types). NH_4Cl was used as a supporting electrolyte on both sides. The electrochemical charge/discharge reactions at the anode and cathode are detailed in Figure 1. The employed redox couple gives a total cell voltage of 0.80 V (see Supplementary Figure 2). Mixtures of 0.25 M $Na_4[Fe(CN)_6]$, 0.25 M $K_4[Fe(CN)_6]$, 0.5 M SPr2V, and 0.5 M NH_4Cl were used as positive and negative electrolytes (i.e., an identical composition of the electrolyte in cathodic and anodic chambers aimed at minimizing the electrolyte crossover). A volume of 18 ml of the mixed electrolyte was added to each compartment, and the solutions were pumped through the system with a flow of 50 mL min^{-1}. Activated SGL Carbon SIGRACELL® graphite felts and gold-plated copper were used as electrodes and current collectors, respectively. The tested membrane area was 5 cm^2. An 857 redox cell test system from Scribner Associates equipped with an 880 impedance analyzer was used as a potentiostat.

Before the test, the through-plane ionic conductivity of the membranes was measured by Electrochemical Impedance Spectroscopy (EIS) in alternating current (AC) mode, with 10 mV amplitude, in the frequency range from 3.2 × 10^7 to 1 Hz, at controlled room temperature (23.5 ± 0.5 °C)[33]. The impedance of the cell

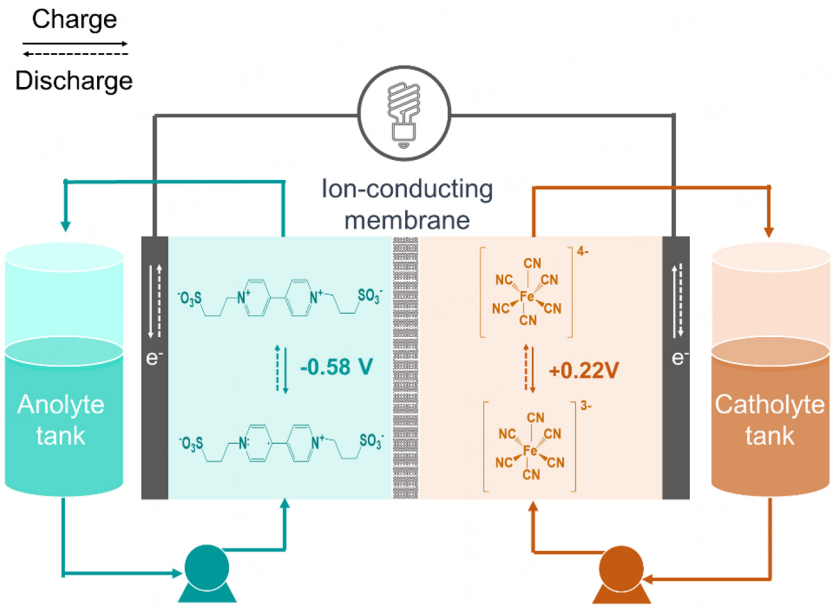

Figure 1. Schematic illustration of the symmetric aqueous organic/organometallic redox flow battery. The half-reduction potentials are referred to as saturated Ag/AgCl reference electrodes.

with and without the membrane was measured and determined from the Nyquist plots and the membrane ionic conductivity (σ) in the working electrolyte was calculated as follows[34],

$$\sigma = \frac{l}{A\,(R_1 - R_2)} \tag{6}$$

where l (cm) is the thickness of the membrane; A (cm^2) is its effective membrane area; and R_1 and R_2 (Ω) are the ohmic resistance of the cell with and without a membrane, respectively.

The cell was subjected to continuous galvanostatic charge/discharge sequences. The charge-discharge cut-off voltages were set at 1.2 and 0.3 V, respectively. The performance was first tested at different current densities (20, 40, 60, and 80 mA cm^{-2}). Then, long cycling tests (up to 200 cycles) were performed at a constant current (60 mA cm^2). The capacity decay during the long cycling test was calculated with respect to the first cycle. The experiments were conducted under a constant flux of argon to avoid side reactions involving oxygen. Before the tests, the membranes were soaked in the supporting electrolyte (0.5 M NH_4Cl) overnight.

RESULTS AND DISCUSSION

Characterization of ion transport nanochannels

The immersion of membranes in solvent-non-solvent baths led to a controllable irreversible swelling of SPEEK polymer chains, which was reflected in a noticeable volumetric expansion of the membranes [Figure 2A]. The degree of swelling relied on the concentration of the solvent used in the solvent-non-solvent bath. In this manner, immersing the membrane in a 40% solvent-non-solvent bath led to a 15% increase in membrane volume compared to its original state, while use of a 50% mixture resulted in a volumetric increase of over 340% compared to the original volume. In this membrane (SPEEK50), an effective modification caused by the swelling of the membrane was visually detected, which may reflect the enlargement of ion transport hydrophilic nanochannels [Figure 2B-D].

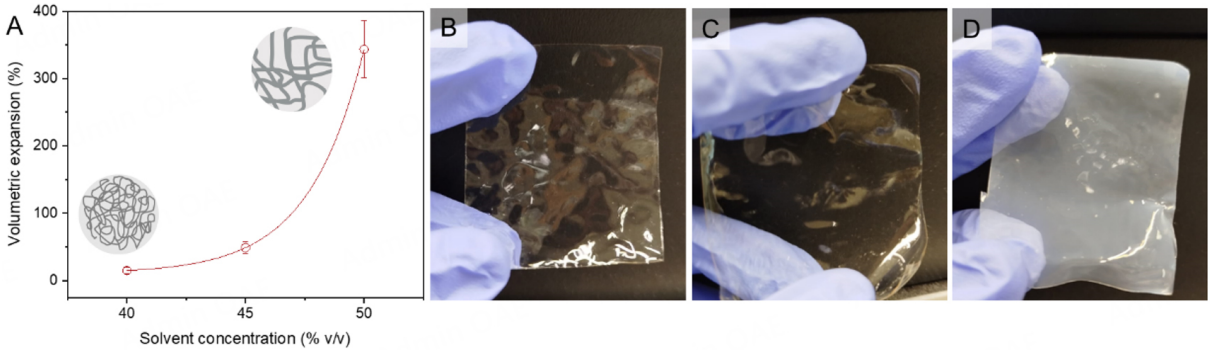

Figure 2. (A) Volumetric expansion of the membrane after the controlled solvent swelling treatment using different solvent concentrations, and digital photos of (B) SPEEK40, (C) SPEEK45, and (D) SPEEK50 membranes.

AFM and SAXS were employed to deeply characterize the transformation of the ion transport nanochannels in the membranes. These techniques can provide essential information about the ionic domains of membranes in contact with liquid electrolytes. Thus, they offer a closer approach to real working conditions (i.e., aqueous electrolyte environment) compared with commonly used techniques, such as N_2 and CO_2 adsorption/desorption[35], and scanning and transmission electron microscopy analyses[36,37], where membrane samples are analyzed in dry conditions.

For AFM study, swollen membranes were kept in glycerol during the analyses to avoid structural changes resulting from the evaporation of water. The AFM phase images served to analyze the hydrophilic and hydrophobic phase distribution at the membrane surface. Figure 3 shows the phase images of the membranes under study, where hydrophilic domains can be distinguished as surface grooves (represented in a darker color), while hydrophobic domains can be recognized as ridges (represented in a lighter color)[38,39]. A considerably homogeneous distribution of the hydrophilic and hydrophobic phase domains was observed for all the membranes. It was observed that SPEEK0 membranes possessed the smallest hydrophilic domains; this fact would, in principle, result in a membrane with lower ionic conductivity and relatively low permeability of redox-active species. From Figure 3B-E, it can be noticed that as the solvent concentration in the treatment increased, the hydrophilic phase domains at the membrane surface were expanded. Thus, the dependence of the dimensions of ion transport nanochannels on the solvent concentration used was verified. In comparison with the reference membrane [Figure 3A], SPEEK40 showed the most similar dimensions of the hydrophilic domains at the membrane surface.

It is worth noting that AFM can only be used to characterize the surface morphology of membranes. We believe that the channel size inside the membrane differs from the hydrophilic domains present on the surface. In fact, according to SAXS results, the channel size inside the membrane was smaller. This is why we used SAXS to determine the channel size throughout the membrane, which has greater relevance to the ion transport characteristics of membranes. However, it is also important to observe changes in the surface morphology of the treated membranes. First, the size of the hydrophilic domains on the surface is quantitatively correlated with the channel size inside the membrane; that is, as the channel size inside the membrane increases, the hydrophilic domains on the surface also grow. Secondly, larger hydrophilic domains on the surface are beneficial for high ion conductivity, while smaller channel sizes inside the membrane contribute to high ion selectivity.

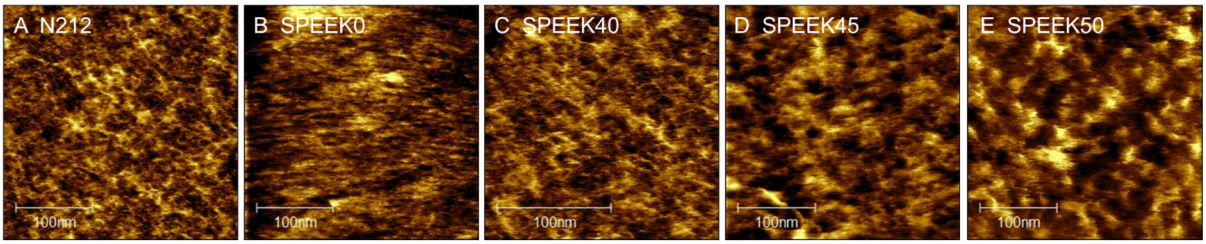

Figure 3. AFM phase images of the membranes under study, (A) N212, (B) SPEEK0, (C) SPEEK40, (D) SPEEK45, (E) SPEEK50.

SAXS has been successfully employed in previous studies to elucidate the phase separation microstructure of Nafion and SPEEK membranes[10,11,38,40-42]. The experimental scheme of SAXS analyses is represented in Supplementary Figure 3A. Besides, a model developed by Gierke *et al.* in[28] was implemented to correlate the distribution of the ion transport clusters (i.e., the lattice plane spacing or *d* spacing) with their actual dimensions. A graphical representation of Gierke´s model is provided in Supplementary Figure 3B. Figure 4A shows the scattering curves of the different membranes analyzed in a water-swollen state. Membranes were prevented from drying during the analysis by tightly sealing the sample holder with Kapton tape. Besides, one of the samples (SPEEK40) was analyzed in a dry state for the sake of comparison [Supplementary Figure 4]. No scattering peak was found in the case of the dry membrane, indicating the shrinkage of the hydrophilic domains, and further corroborating the preservation of water in the rest of the samples during the analyses.

In the case of N212 membranes, the extremely hydrophobic perfluorinated polymer in contrast with the hydrophilicity of acidic sulfonic groups results in a well-defined nanophase separation as sulfonic groups tend to form clusters. In the SAXS analysis, this microstructure is reflected by two distinct scattering peaks [Figure 4A]. The first peak shows up at low *q* values and corresponds to the hydrophobic domains of the polymer backbone. The second peak arises at higher *q* values and belongs to the hydrophilic domains of the ionomer clusters[41]. In contrast, no peak was found in the case of the untreated SPEEK0 membrane, which is in good agreement with the literature reports, and reflects a low electron density contrast between the ionomer clusters and the PEEK polymer backbone (too low to produce a scattering peak)[10,11]. This scattering behavior indicates the conformation of small SO_3^- clusters. In turn, the presence of small clusters arises from the lower acidity of the sulfonate groups due to the less polarizing alkyl chain of PEEK, and from the higher rigidity of the PEEK polymer backbone that could impede the rearrangement of SO_3^- groups. The small SO_3^- clusters lead to narrow ion transport channels, as corroborated by AFM images [Figure 3B]. According to the literature[40], these narrow channels could be branched and possess multiple dead ends, which could slow down the ion transport in comparison with Nafion.

However, after controlled swelling, a single scattering peak emerged in the modified SPEEK membranes, which may arise from a greater electron density contrast between larger water-filled ionomer clusters and the polymer backbone, resulting from the strengthened phase separation between the hydrophobic polymer backbone and the hydrated hydrophilic ionic clusters after swelling[11]. Previous research has attributed this peak in SPEEK membranes to the ionomer domains[10,11]. Yet, the presence of a single peak in the modified SPEEK membranes indicates that the hydrophilic and hydrophobic domains are not so well defined as in the case of Nafion membranes, again, as a consequence of the lack of the extremely electronegative fluorine atoms in the polymer. The presence of the scattering peak also indicates that the water content of the membranes was preserved during SAXS analyses. This was verified by the comparison of the scattering curves of water-swollen and dry SPEEK40 membranes (see Supplementary Figure 2), provided that no scattering peaks were found in the dry membrane.

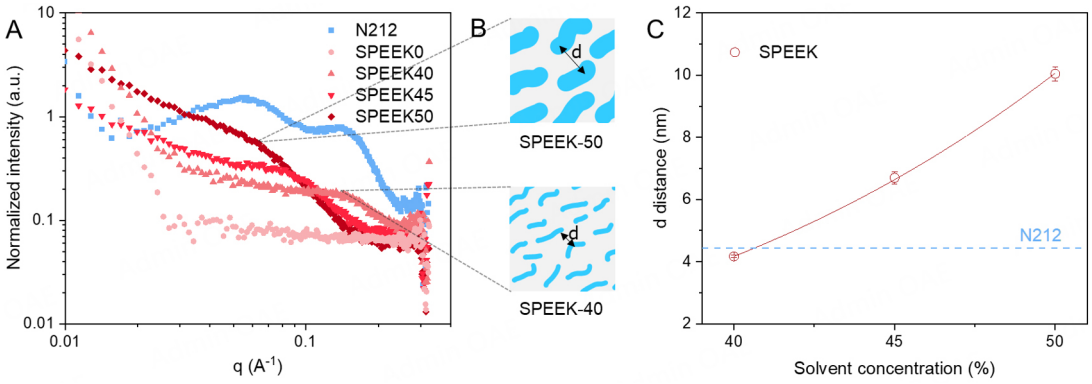

Figure 4. (A) Scattering curves of water-swollen membranes by SAXS, (B) illustration of ion-transport channel modification due to controlled irreversible swelling treatment, (C) lattice plane spacing (*d* distance) calculated from the scattering peaks and relation with the solvent concentration used in the treatment.

According to Bragg´s law, the peak position of the ionomer cluster is related to the distance between two adjacent hydrophilic domains, referred to as *d* distance, with lower *q* values indicative of a larger *d* distance. It was observed that the ionomer peaks of solvent-treated SPEEK membranes were displaced to lower *q* values as the concentration of the solvent increased, thus indicating larger *d* distances [Figure 4A and B]. The *d* distances for N212 and solvent-treated SPEEK membranes were calculated according to the corresponding *q* values (detailed in Supplementary Table 1), and are displayed in Figure 4C. A smooth, almost linear correlation between the solvent concentration and the *d* distance was observed. These results verified that the microstructure of the membranes was finely modified by the controlled-swelling treatment, as corroborated by AFM images [Figure 3C-E].

Using Supplementary Equations 1-4 reported before by Gierke *et al.* in[28], and based on experimental dry membrane density, water absorption, and *d* distances, the diameters of the ionomer clusters (d_c) were calculated, and the results are summarized in Table 1. These equations approximated the ionomer clusters to spheres with a simple cubic lattice distribution based on *d* distance. Although the structural model of the ionomer clusters is yet under scientific discussion[10,11,38,40-42], the Gierke model[28] is a generally accepted approximation that served us to estimate an approximated average size of the ionic clusters. As illustrated in Figure 4B, a correlation between the *d* distance and the size of the clusters (d_c) can be found in the data displayed in Table 1. The d_c value obtained for the N212 membrane falls within the range of those measured by Gierke *et al.* for different Nafion membranes (2.5-5.1 nm, depending on the equivalent weight, counter ion and pretreatment used)[28]. The modified membrane SPEEK40 has the most similar size of the ionomer clusters compared to N212. In the case of SPEEK45 and SPEEK50, larger clusters can be found, which is in concordance with AFM results previously presented. The large water absorption and cluster size of SPEEK50 suggests that different clusters were merged and interconnected.

In sum, SAXS and AFM characterization of swollen ion transport channels served us to verify that the size of the ionomer clusters was customized at a nanometric scale by adjusting the concentration of the solvent.

Ionic conductivity and permeability

The apparent porosity [Figure 5A] is directly related to the swelling behavior of the membranes. Thus, in concordance with the volumetric expansion of the membranes, the apparent porosity raised with the concentration of the solvent used in the treatments [Figure 2A]. In line with previously presented AFM and SAXS results, the sizeable increase of the apparent porosity indicates the formation of significantly larger

Table 1. Calculation of approximated ionomer cluster size (d_c) according to Supplementary Equations 1-4, for averaged equivalent weights (M_{eq}) of 1,020 g eq^{-1} for N212, and 580 g eq^{-1} for SPEEK (57% sulfonation degree). ρ,dry membrane density; Δm water absorption (mass)

Membrane	ρ dry membrane (g cm^{-3})	Δm (g g^{-1})	*d* distance (nm)	d_c (nm)
N212	1.97	0.14	4.4	3.28
SPEEK40	1.36	0.33	4.2	3.50
SPEEK45	1.36	0.38	6.7	5.80
SPEEK50	1.36	3.46	10.0	11.69

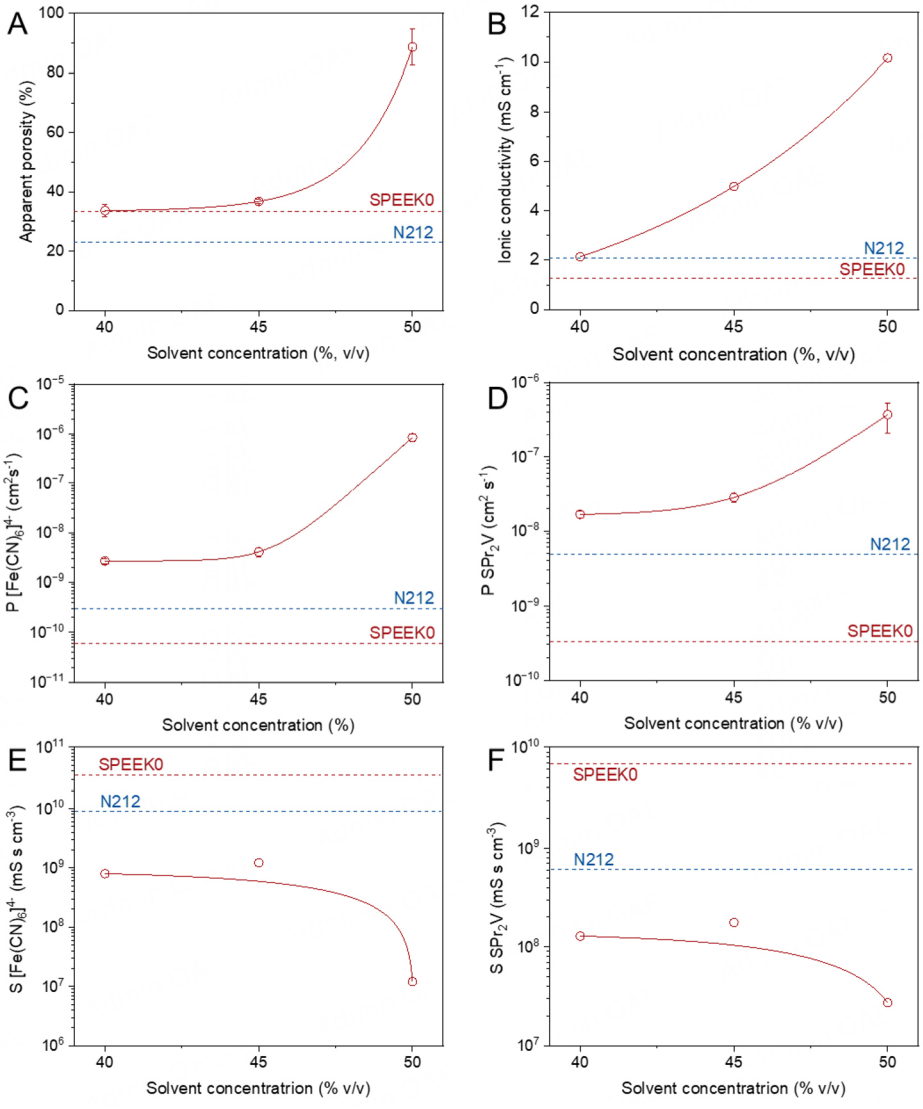

Figure 5. (A) Apparent porosity, (B) ionic conductivity in the symmetric electrolyte, (C) permeability to ferrocyanide, (D) permeability to SPr_2V, (E) selectivity to ferrocyanide, (F) selectivity to SPr_2V.

water-filled hydrophilic ion transport channels. Consequently, the ionic conductivity of the modified membranes exhibited a substantial boost compared to SPEEK0 (1.3 mS cm^{-1}), reaching almost an eight-fold increase in the case of the SPEEK50 membrane (10.2 mS cm^{-1}) [Figure 5B]. SPEEK40 and N212 membranes

presented a very similar ionic conductivity, as predicted by AFM and SAXS results, due to the conformation of ionic domains of very similar sizes. Interestingly, the larger water absorption and lower equivalent weight of SPEEK40 [i.e., higher ion-exchange capacity (IEC), Table 1] did not contribute to attaining a greater ionic conductivity at the same size of the ionic clusters, in comparison with N212. This may be attributed to the higher acidity of the sulfonic acid groups and more concentrated ionic clusters formed due to the phase separation in the Nafion membrane, both of which contribute to faster mobility of ions through the membrane. In the cases of SPEEK45 and SPEEK50, the ionic conductivity of the reference membrane was surpassed, due to the presence of larger ionomer clusters. It can be noticed that the ionic conductivity of the reference membrane (N212) is significantly lower than in the case of using a sulfuric acid media (typically around 25 mS cm^{-1} in 1 M sulfuric acid). This is a consequence of the lower conductivity of the near-neutral pH electrolyte in comparison with 1 M H_2SO_4 (95 ± 2 and 265 ± 5 mS cm^{-1}, respectively), which in turn arises from the larger hydrodynamic radius (slower mobility) of the charge carriers in the electrolyte media (K^+, Na^+ and NH_4^+) with respect to H^+[43].

Regarding the permeability of the membranes to the redox-active molecules, the SPEEK0 membrane showed an ultra-low permeability, due to the presence of very narrow ion transport channels in the membrane. In fact, SPEEK0 reached one order of magnitude lower permeability than N212 for both active materials under study [Figure 5C and D]. Increasing the solvent concentration led to a faster permeation of redox-active materials through the membranes, evidencing the enlargement of ion transport channels. As a result, SPEEK50 membranes exhibited a relatively high permeability, two and three orders of magnitude larger than the reference membrane for SPr_2V and ferrocyanide ions, respectively. This relatively large permeability would induce cycling inefficiencies and electrolyte unbalance in the RFB. In general, the permeability of the organic SPr_2V (uncharged at neutral state) is one order of magnitude larger than the permeability of sodium and potassium ferrocyanide salts, indicating that charge repulsion is an effective mechanism avoiding the permeation of negatively charged species across cation-exchange membranes.

Membrane selectivity is defined as the ratio between ionic conductivity and the permeability of redox materials. Therefore, this parameter indicates how well-balanced these performance-determining parameters are. It was found that the untreated SPEEK0 membrane possessed the best selectivity [Figure 5E and F], even higher than N212, owing to the ultra-low permeability this membrane exhibited. The selectivity then declines with increasing concentration of the solvent due to increased permeability to the redox materials. A predominant effect of permeability on selectivity is clearly observed in the trends of Figure 5C and D *vs.* Figure 5E and F, as it is declined even if a continuous increase of the conductivity is observed [Figure 5B] (i.e., selectivity only drops when permeability increases). Among the modified membranes, SPEEK45 showed the best selectivity due to the combination of a significantly enhanced ionic conductivity (5.0 mS cm^{-1}) and a moderate permeability of the redox molecules (2.82 × 10^{-8} and 4.10 × 10^{-9} cm^2 s^1, for SPr_2V and ferrocyanide salts, respectively).

Mechanical strength

Proper mechanical strength is essential to ensure processability and durability of membranes for practical applications. SPEEK polymer dense films are well known for their excellent mechanical stability, which surpasses that of Nafion polymer membranes of similar thickness[6]. The stress-strain curves obtained in this study corroborated this fact, as shown in Figure 6A. It can be noticed that the mechanical strength of SPEEK membranes was reduced with increasing solvent concentration used in the swelling treatments (from 29.7 MPa of SPEEK0 membranes to 6.7 MPa in the case of SPEEK50 membranes). Despite that, except for SPEEK50 membranes, solvent-treated SPEEK membranes showed greater tensile strength than N212 (16.5 MPa). The reduction of the tensile strength with the increase in the concentration of the solvent is a consequence of the sizeable expansion of water-filled ion transport channels in solvent-treated

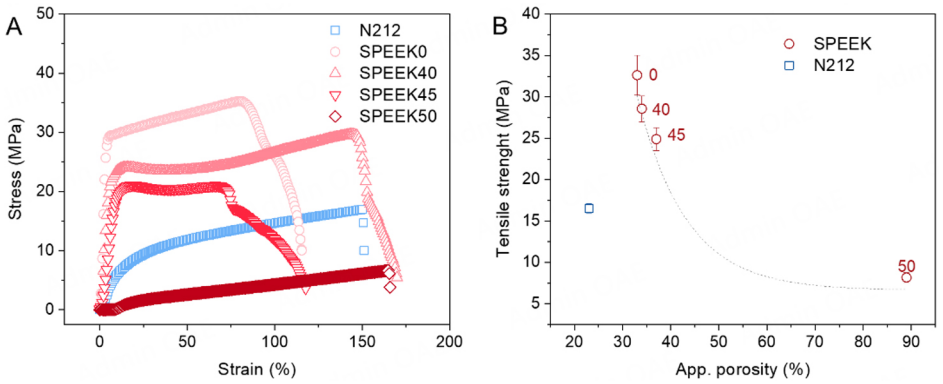

Figure 6. Mechanical properties of all the membranes tested, (A) stress-strain curves, (B) relationship between tensile strength and apparent porosity.

membranes[24,25]. Figure 6B shows the relation between mechanical strength and apparent porosity, which agrees well with previous studies on porous membranes[24,34].

Single cell performance

In this study, a symmetric configuration of an organic/organometallic (SPr_2V and sodium and potassium ferrocyanide) mixture was used to test the cycling efficiency of the membranes. This implies that both electrolytes have the same composition in the uncharged state of the battery; thus, chemical and electrochemical potentials across the cell are minimized (i.e., transport driving forces), resulting in the mitigation of undesired crossover effects[26,44]. It is worth noting that although the chemical stability is not as high as perfluorinated polymers, it could be promising for near-neutral pH and lower oxidation potential of the electrolytes as used in this work.

The performance of the modified SPEEK45 (i.e., the membrane showing the best combination of transport and mechanical properties) was tested in the RFB and the results were compared with the N212 membrane. The performance of the membranes in terms of cell efficiency was first analyzed at different current densities [Figure 7A]. SPEEK45 membranes showed a higher voltage efficiency (VE) than N212 membranes at all current densities tested (e.g., 72.5% and 68.1% respectively, at 60 mA cm^{-2},), this is ascribed to the enhanced ionic conductivity of the modified membrane. At the lowest current density (20 mA cm^{-2}), the longer charge-discharge steps expose the difference in permeability of SPEEK45 and N212, which is ultimately reflected in the CE. Thus, SPEEK45 shows a slightly lower CE. As typically observed, the VE and EE showed a steady decline with increasing current densities due to greater ohmic losses and concentration polarization effects[45]. Using a similar chemistry (i.e., a symmetric cell configuration with 0.5 M $(NH_4)_4[Fe(CN)_6]$/$(SPr)_2V$ in 1.0 M NH_4Cl electrolyte), a Selemion CSO cation-exchange membrane reached 75% EE at 60 mA cm^{-2} in[26]. The slightly higher efficiency of their setup could arise from the higher conductivity provided by $(NH_4)_4[Fe(CN)_6]$ and the supporting electrolyte used.

Besides, SPEEK45 maintained stable efficiency over 200 charge-discharge cycles at 60 mA cm^2 [Figure 7B], consistently achieving a higher EE than the cell using the N212 membrane throughout the test (70.8% and 65.4% after 200 cycles, respectively). The normalized capacity was calculated, as given in Figure 7C, by $Normalized\ Capacity = \left(\frac{C_{n,disch.}}{C_{1,disch.}}\right) \times 100\%$, with $C_{n,disch.}$ being the discharge capacity at n cycle in Ah and $C_{1,disch.}$ being the discharge capacity at the first cycle. Regarding the capacity retention, both batteries using SPEEK45 and N212 membranes showed very similar trends, presenting a gradual capacity decay during the experiments. Capacity decay in this work is defined as

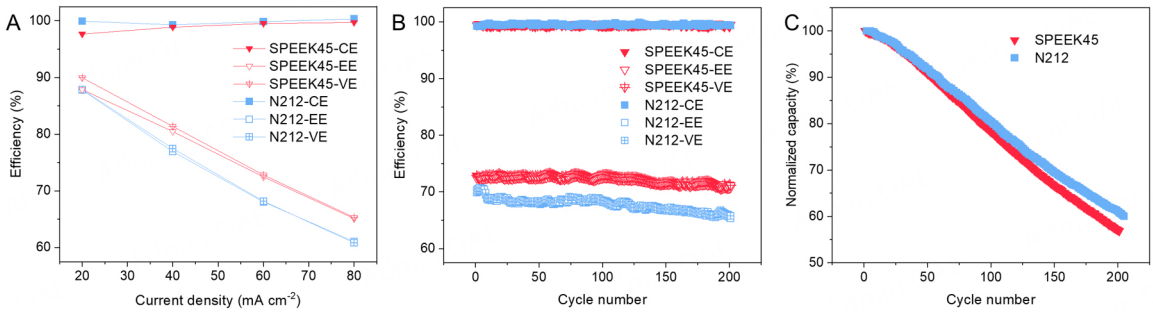

Figure 7. Single cell battery performance using SPEEK45 and N212 membranes (A) cell efficiencies at different current densities, (B) long-term cell efficiencies, and (C) evolution of the normalized capacity during long-term cycling.

$Capacity\ decay = \left(\frac{C_{1,disch.} - C_{n,disch.}}{C_{1,disch.}}\right) \times 100\%$. After 200 cycles, a capacity fade of 43.2% and 40% was observed in cells using SPEEK45 and N212 membranes, respectively (0.21% and 0.18% capacity fade per hour, respectively). However, the cyclic voltammetry (CV) analysis of the positive and negative electrolytes after 200 charge-discharge cycles did not reveal significant differences in respect to the initial electrolyte [Supplementary Figure 5]. No new peaks were observed, nor was there a great difference in peak intensity, indicating that the degradation of the electrolyte might not be the main reason for the capacity decay. Since the capacity decay for both membranes is similar, the crossover of redox-active species in more permeable SPEEK45 membranes (one order of magnitude higher permeability to both redox mediators than N212 membrane) was substantially reduced owing to the use of a symmetric cell configuration[44]. In this case, the significant capacity decay of both batteries using SPEEK45 and N212 membranes may result from the severe electrolyte migration from the cathode to the anode, which was observed during the tests. Nevertheless, it was reported that the chemical stability of the anodic active material could also be an issue in the case of the presence of small oxygen traces[46,47].

These results demonstrated that finely controlled irreversible swelling is a promising strategy for achieving nanometric control over the ion transport nanochannels, attaining a well-balanced performance and cost in fluorine-free SPEEK membranes, and promoting a high EE in some RFBs. Yet, it is important to concede that the increase of permeability to the redox-active molecules in solvent-swollen membranes could pose a challenge for their large-scale implementation in various RFBs. Indeed, the loss of selectivity is a general bottleneck of all forms of microporous membranes. In this context, novel strategies still need to be developed that focus on reducing the transport channel size or enhancing charge repulsion. Asymmetric microporous structures having a thin dense surface present a bright future to reduce crossover of microporous membranes[48]. In the case of solvent-swollen membranes, coating the membranes with an ultrathin dense layer could potentially yield positive results[49]. Besides, the modification of battery chemistry, such as using polymeric redox-active materials[50], or symmetric electrolyte compositions, as in the case of the present work, are other avenues to mitigate crossover in membranes having wide ion transport channels. Lastly, it is worth noting that near-neutral pH FBs provide a less harsh environment than vanadium-based systems, making the employed chemistry more suitable for the implementation of non-perfluorinated membranes.

CONCLUSIONS

SPEEK is an excellent candidate to replace Nafion materials in some RFBs based on its fluorine-free nature, mechanical robustness, processability, and remarkably low cost. Controlled irreversible swelling represents a facile and economic method to finely tune the microstructure of SPEEK at a nanometric scale, creating

wide and well interconnected ion-transport channels. The size of the ion transport channels was successfully investigated in wet conditions, revealing that the channels were enlarged proportionally to the solvent concentration used in the treatment. Consequently, the ionic conductivity of solvent-treatment SPEEK membranes was significantly boosted. Thus, the modified SPEEK45 membrane exhibited higher EEs than the N212 membrane across the tested range of current densities, maintaining stable performance over 200 cycles, and demonstrating a similar capacity retention as the N212 membrane. Overall, controlled irreversible swelling is a facile membrane technology that enables nanometric customization of ion transport channels in polymer membranes. This allows for tailored conductivity and selectivity based on the redox pairs, resulting in cost-effective, high-performance membranes suitable for various FBs.

DECLARATIONS

Acknowledgments

We gratefully acknowledge the exceptional technical support María Jauregui Vicente and Asier Uria Martinez provided.

Authors' contributions

Made substantial contributions to conception and design of the study and performed data analysis and interpretation: Lejarazu-Larrañaga, A.; Jiang, F.; Sánchez-Díez, E.; Zhang, Y.; Bobrikov, I.; Ortiz-Vitoriano, N.

Performed data acquisition and provided administrative, technical, and material support: Jiang, F.; Lejarazu-Larrañaga, A.; Marquinez, N.; Bobrikov, I.; Zhang, Y.

Prepared the manuscript: Lejarazu-Larrañaga, A.; Sánchez-Díez, E.; Zhang, Y.; Bobrikov, I.; Ortiz-Vitoriano, N.

Supervised this project: Jiang, F.

Availability of data and materials

The data supporting our findings can be found in the Supplementary Material.

Financial support and sponsorship

Ortiz-Vitoriano, N. acknowledges the grant RYC2020-030104-I funded by MCIN/AEI/10.13039/501100011033 and by "ESF Investing in your future".

Conflicts of interest

All authors declared that there are no conflicts of interest.

Ethical approval and consent to participate

Not applicable.

Consent for publication

Not applicable.

REFERENCES

1. Sánchez-Díez, E.; Ventosa, E.; Guarnieri, M.; et al. Redox flow batteries: status and perspective towards sustainable stationary energy storage. *J. Power. Sources.* **2021**, *481*, 228804. DOI
2. European Chemicals Agency. Annex XV-restriction report proposal for per- and polyfluoroalkyl substances (PFASs). Helsinki, Finland: European Chemicals Agency; 2023. Available from: https://echa.europa.eu/restrictions-under-consideration/-/substance-rev/

72301/term [Last accessed on 19 Feb 2025]
3. Minke, C.; Turek, T. Economics of vanadium redox flow battery membranes. *J. Power. Sources.* **2015**, *286*, 247-57. DOI
4. Janoschka, T.; Martin, N.; Martin, U.; et al. An aqueous, polymer-based redox-flow battery using non-corrosive, safe, and low-cost materials. *Nature* **2015**, *527*, 78-81. DOI
5. Thiam, B. G.; El, M. A.; Vaudreuil, S. An overview on the progress and development of modified sulfonated polyether ether ketone membranes for vanadium redox flow battery applications. *High. Perform. Polym.* **2022**, *34*, 131-48. DOI
6. Mahimai B, Sivasubramanian G, Sekar K, Kannaiyan D, Deivanayagam P. Sulfonated poly(ether ether ketone): efficient ion-exchange polymer electrolytes for fuel cell applications-a versatile review. *Mater. Adv.* **2022**, *3*, 6085-95. DOI
7. Schwenzer, B.; Zhang, J.; Kim, S.; Li, L.; Liu, J.; Yang, Z. Membrane development for vanadium redox flow batteries. *ChemSusChem* **2011**, *4*, 1388-406. DOI
8. Zhang, L.; Zhang, S.; Li, E.; Zhao, L.; Zhang, S. Sulfonated poly(ether ether ketone) membrane for quinone-based organic flow batteries. *J. Membr. Sci.* **2019**, *584*, 246-53. DOI
9. Chu, B.; Hsiao, B. S. Small-angle X-ray scattering of polymers. *Chem. Rev.* **2001**, *101*, 1727-61. DOI PubMed
10. Yang, B.; Manthiram, A. Comparison of the small angle X-ray scattering study of sulfonated poly(etheretherketone) and Nafion membranes for direct methanol fuel cells. *J. Power. Sources.* **2006**, *153*, 29-35. DOI
11. Mendil-Jakani, H.; Zamanillo, L. I.; Mareau, V. H.; Gonon, L. Optimization of hydrophilic/hydrophobic phase separation in sPEEK membranes by hydrothermal treatments. *Phys. Chem. Chem. Phys.* **2017**, *19*, 16013-22. DOI PubMed
12. Qian, P.; Zhou, W.; Zhang, Y.; Chao, D.; Song, M. Review and perspectives of sulfonated poly(ether ether ketone) proton exchange membrane for vanadium flow batteries. *Energy. Fuels.* **2023**, *37*, 17681-707. DOI
13. Brush, D.; Danilczuk, M.; Schlick, S. Phase separation in sulfonated poly(ether ether ketone) (SPEEK) ionomers by spin probe ESR: effect of the degree of sulfonation and water content. *Macromolecules* **2015**, *48*, 637-44. DOI
14. Yuan, Z.; Li, X.; Hu, J.; Xu, W.; Cao, J.; Zhang, H. Degradation mechanism of sulfonated poly(ether ether ketone) (SPEEK) ion exchange membranes under vanadium flow battery medium. *Phys. Chem. Chem. Phys.* **2014**, *16*, 19841-7. DOI
15. Xiong, P.; Zhang, L.; Chen, Y.; Peng, S.; Yu, G. A chemistry and microstructure perspective on ion-conducting membranes for redox flow batteries. *Angew. Chem. Int. Ed.* **2021**, *60*, 24770-98. DOI
16. Ye, C.; Tan, R.; Wang, A.; et al. Long-life aqueous organic redox flow batteries enabled by amidoxime-functionalized ion-selective polymer membranes. *Angew. Chem. Int. Ed.* **2022**, *61*, e202207580. DOI PubMed PMC
17. Tan, R.; Wang, A.; Ye, C.; et al. Thin film composite membranes with regulated crossover and water migration for long-life aqueous redox flow batteries. *Adv. Sci.* **2023**, *10*, e2206888. DOI PubMed PMC
18. Chen, D.; Li, D.; Li, X. Hierarchical porous poly (ether sulfone) membranes with excellent capacity retention for vanadium flow battery application. *J. Power. Sources.* **2017**, *353*, 11-8. DOI
19. Che, X.; Zhao, H.; Ren, X.; et al. Porous polybenzimidazole membranes with high ion selectivity for the vanadium redox flow battery. *J. Membr. Sci.* **2020**, *611*, 118359. DOI
20. Wang, F.; Zhang, Z.; Jiang, F. Dual-porous structured membrane for ion-selection in vanadium flow battery. *J. Power. Sources.* **2021**, *506*, 230234. DOI
21. Zhang, J.; Lejarazu-larrañaga, A.; Yang, F.; et al. Tailoring porous structure in non-ionic polymer membranes using multiple templates for low-cost iron-lead single-flow batteries. *Energy. Mater.* **2024**, *4*, 400042. DOI
22. Zhai, S.; Jia, X.; Lu, Z.; et al. Highly ion selective composite proton exchange membranes for vanadium redox flow batteries by the incorporation of UiO-66-NH_2 threaded with ion conducting polymers. *J. Membr. Sci.* **2022**, *662*, 121003. DOI
23. Xia, Y.; Wang, Y.; Cao, H.; et al. Rigidly and intrinsically microporous polymer reinforced sulfonated polyether ether ketone membrane for vanadium flow battery. *J. Membr. Sci.* **2022**, *653*, 120517. DOI
24. Jiang, F.; Zhang, Y.; Wang, F.; Zhou, X.; Liao, W. Finely controlled swelling: a shortcut to construct ion-selective channels in polymer membranes. *Polymer* **2021**, *225*, 123793. DOI
25. Jiang, F.; Xue, R. Ion-selective membranes fabricated using finely controlled swelling of non-ionic fluoropolymer for redox flow batteries. *Batteries* **2023**, *9*, 545. DOI
26. Luo, J.; Hu, B.; Debruler, C.; et al. Unprecedented capacity and stability of ammonium ferrocyanide catholyte in pH neutral aqueous redox flow batteries. *Joule* **2019**, *3*, 149-63. DOI
27. Jiang, M.; Candeloro, D.; Mahesh, J. M. Hydrophilic hollow fiber ultrafiltration membranes that include a hydrophobic polymer and a method of making these membranes. WO2002076593A1. Available from: https://patents.google.com/patent/WO2002076593A1/en [Last accessed on 19 Feb 2025]
28. Gierke, T. D.; Munn, G. E.; Wilson, F. C. The morphology in nafion perfluorinated membrane products, as determined by wide- and small-angle X-ray studies. *J. Polym. Sci. Polym. Phys. Ed.* **1981**, *19*, 1687-704. DOI
29. Xue, R.; Jiang, F.; Wang, F.; Zhou, X. Towards cost-effective proton-exchange membranes for redox flow batteries: a facile and innovative method. *J. Power. Sources.* **2020**, *449*, 227475. DOI
30. Hu, B.; Hu, M.; Luo, J.; Liu, T. L. A stable, low permeable TEMPO catholyte for aqueous total organic redox flow batteries. *Adv. Energy. Mater.* **2022**, *12*, 2102577. DOI
31. Kingsbury, R. S.; Zhu, S.; Flotron, S.; Coronell, O. Microstructure determines water and salt permeation in commercial ion-exchange membranes. *ACS. Appl. Mater. Interfaces.* **2018**, *10*, 39745-56. DOI PubMed
32. Krowne, C. M. Physics, electrochemistry, chemistry, and electronics of the vanadium redox flow battery by analyzing all the

governing equations. *Phys. Chem. Chem. Phys.* **2024**, *26*, 2823-62. DOI PubMed

33. Ye, C.; Wang, A.; Breakwell, C.; et al. Development of efficient aqueous organic redox flow batteries using ion-sieving sulfonated polymer membranes. *Nat. Commun.* **2022**, *13*, 3184. DOI PubMed PMC
34. Zhou, X.; Xue, R.; Zhong, Y.; Zhang, Y.; Jiang, F. Asymmetric porous membranes with ultra-high ion selectivity for vanadium redox flow batteries. *J. Membr. Sci.* **2020**, *595*, 117614. DOI
35. Garcia-Vasquez, W.; Dammak, L.; Larchet, C.; Nikonenko, V.; Pismenskaya, N.; Grande, D. Evolution of anion-exchange membrane properties in a full scale electrodialysis stack. *J. Membr. Sci.* **2013**, *446*, 255-65. DOI
36. Folkertsma, L.; Zhang, K.; Czakkel, O.; et al. Synchrotron SAXS and impedance spectroscopy unveil nanostructure variations in redox-responsive porous membranes from poly(ferrocenylsilane) poly(ionic liquid)s. *Macromolecules* **2017**, *50*, 296-302. DOI
37. He, G.; Li, Z.; Zhao, J.; et al. Nanostructured ion-exchange membranes for fuel cells: recent advances and perspectives. *Adv. Mater.* **2015**, *27*, 5280-95. DOI
38. Choi, S.; Jin, K. S. Ex situ aging effect on sulfonated poly(ether ether ketone) membrane: hydration-dehydration cycling and hydrothermal treatment. *J. Energy. Chem.* **2022**, *70*, 583-92. DOI
39. Oh, K.; Bae, I. Engineered membrane-electrode interface for hydrocarbon-based polymer-electrolyte-membrane fuel cells via solvent-vapor-annealed deposition. *ACS. Appl. Nano. Mater.* **2019**, *2*, 3857-63. DOI
40. Kreuer, K. D. On the development of proton conducting polymer membranes for hydrogen and methanol fuel cells. *J. Membr. Sci.* **2001**, *185*, 29. DOI
41. Mensharapov, R. M.; Ivanova, N. A.; Spasov, D. D.; Grigoriev, S. A.; Fateev, V. N. SAXS investigation of the effect of freeze/thaw cycles on the nanostructure of nafion® membranes. *Polymers* **2022**, *14*, 4395. DOI PubMed PMC
42. Mendil-Jakani, H.; Zamanillo, L. I.; Legrand, P. M.; Mareau, V. H.; Gonon, L. A new interpretation of SAXS peaks in sulfonated poly(ether ether ketone) (sPEEK) membranes for fuel cells. *Phys. Chem. Chem. Phys.* **2014**, *16*, 11228-35. DOI PubMed
43. Caianiello, C.; Arenas, L. F.; Turek, T.; Wilhelm, R. Characterization of an aqueous flow battery utilizing a hydroxylated tetracationic viologen and a simple cationic ferrocene derivative. *Adv. Energy. Sustain. Res.* **2023**, *4*, 2300077. DOI
44. Potash, R. A.; Mckone, J. R.; Conte, S.; Abruña, H. D. On the benefits of a symmetric redox flow battery. *J. Electrochem. Soc.* **2016**, *163*, A338-44. DOI
45. Song, Y.; Li, X.; Yan, C.; Tang, A. Uncovering ionic conductivity impact towards high power vanadium flow battery design and operation. *J. Power. Sources.* **2020**, *480*, 229141. DOI
46. Rubio-Presa, R.; Lubián, L.; Borlaf, M.; Ventosa, E.; Sanz, R. Addressing practical use of viologen-derivatives in redox flow batteries through molecular engineering. *ACS. Mater. Lett.* **2023**, *5*, 798-802. DOI PubMed PMC
47. Jin, S.; Fell, E. M.; Vina-Lopez, L.; et al. Near neutral pH redox flow battery with low permeability and long-lifetime phosphonated viologen active species. *Adv. Energy. Mater.* **2020**, *10*, 2000100. DOI
48. Gubler, L. Membranes and separators for redox flow batteries. *Curr. Opin. Electrochem.* **2019**, *18*, 31-6. DOI
49. Austing JG, Nunes Kirchner C, Komsiyska L, Wittstock G. Layer-by-layer modification of Nafion membranes for increased life-time and efficiency of vanadium/air redox flow batteries. *J. Membr. Sci.* **2016**, *510*, 259-69. DOI
50. Lai, Y. Y.; Li, X.; Zhu, Y. Polymeric active materials for redox flow battery application. *ACS. Appl. Polym. Mater.* **2020**, *2*, 113-28. DOI